Inorganic Chemistry

pubs.acs.org/IC

Article

Three Phases of Basic Zirconium and Hafnium Hydroxohalides

James A. Sommers, Jenn M. Amador, Lauren B. Fullmer, Danielle C. Hutchison, T. Wesley Surta, Oksana Ostroverkhova, May Nyman, and Douglas A. Keszler*

Cite This: https://doi.org/10.1021/acs.inorgchem.3c00633

Read Online

ACCESS | Metrics & More | Article Recommendations | Supporting Information

ABSTRACT: Aqueous solutions of zirconium and hafnium (M) halides (X) with atomic ratios α = X/M near 1 form glasses on evaporation. Herein, we describe the preparation and properties of these glasses and discuss the nature of the crystal−glass equilibria beyond the pure glass compositions. Small- and wide-angle X-ray scattering (SWAXS) studies reveal increased polymerization as α decreases from 2 to 1. The glasses are found to be much denser than their crystalline counterparts. Crystals forming in contact with glasses retain the well-known Zr-tetrameric hydroxo cluster unit with hydroxide compensating for the lowered halide content. We find that the chemical formulas for all of the solid hydroxohalides may be described by the single parameter α, according to the formula $M(OH)_{4-\alpha}X_\alpha\cdot(4\alpha - 1)H_2O$. This description is valid for the crystalline chloride ($MOX_2\cdot 8H_2O = M(OH)_2X_2\cdot 7H_2O$), the glassy solids with $\alpha < 2$, and hydrolyzed products ($\alpha \approx 0.5$). The water content is also determined by α with hydroxide−hydrogen bonding replacing halide−hydrogen bonding as α decreases. A Eu^{3+}-doped Zr,Cl glass exhibits photoluminescence transitions $^5D_0 \rightarrow {}^7F_n$ (n = 1, 2, and 4) of Eu^{3+}, illustrating the asymmetric nature of the dopant sites in the glass.

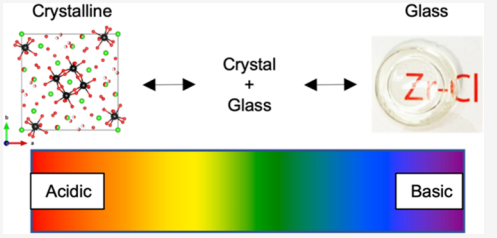

1. INTRODUCTION

Zirconium oxide chloride octahydrate ($ZrOCl_2\cdot 8H_2O$, ZOC) is the basis of nearly all practical chemistry of zirconium materials. It is extracted from zircon sand, $ZrSiO_4$, either by carbochlorination or caustic fusion. It is also a feedstock for separation of hafnium from zirconium by liquid−liquid extraction from which hafnium oxide chloride (HOC) may be obtained after several steps.[1] The common formulation and nomenclature of ZOC and HOC are misleading, as Clearfield and Vaughan[2] established the existence of the hydroxo-bridged tetramer $[Zr_4(OH)_8]^{8+}$ from a crystal-structure determination of ZOC. The tetrameric structure $[Hf_4(OH)_8]^{8+}$ is also found in HOC, and in each material, eight chloride anions balance the cationic charge. The same formulas and properties exist for the corresponding bromides and iodides, which Blumenthal[3] has collectively coined halogenides.

The hydroxohalide compositions may be modified by replacement of hydroxide for halide according to the formulation $M(OH)_{4-\alpha}X_\alpha\cdot(4\alpha - 1)H_2O$ ($0 < \alpha < 2$). Hydroxohalides with $\alpha < 2$ are deficient in Cl and are considered to be basic, as OH^- replaces Cl^-. Hydroxohalides of Zr with α near 1 for Cl, Br, and I exist as glasses, but they are rarely encountered in the literature beyond Blumenthal's work. Blumenthal cites a report from 1875[4] quoting a formula of "$ZrOOHCl\cdot nH_2O$". The term "glass" as used herein describes materials that are observed to be monolithic, transparent, and displaying only broad and weak X-ray diffraction peaks. It is remarkable that compositions so near such an important reagent as ZOC remain uninvestigated. No results appear to have been reported for glasses containing Hf nor any halogens except Cl. Thus, we have an opportunity to investigate the basic hydroxohalides of zirconium and hafnium across a range of α. Herein, we focus on the nature of amorphous compositions, relying on the characteristics of their solution precursors and crystalline analogues to describe their compositions and structures.

2. RESULTS AND DISCUSSION

2.1. Glass Properties. The methods to prepare solutions, ~1 M in metal and $\alpha \approx 1$, are described in the Supporting Information. Conditions for evaporation were those prevailing in the laboratory, which typically ranged from about 20 to 30 °C, and about 20 to 50% relative humidity (RH). Samples were 1−5 mM in the metal content, about 5 mL in volume. When left for water evaporation for a period of 1−4 days, depending on the initial volume, ambient temperature, and RH, solutions lose about 80% of their mass and become increasingly viscous then rigid to yield transparent, hard disks of the type shown in Figure 1. Weight loss was measured until it was no longer monotonic and followed daily variations in RH. Evaporation in a hydrophobic container, such as a polypropylene beaker, eases recovery, as the disks shrink away

Received: February 25, 2023

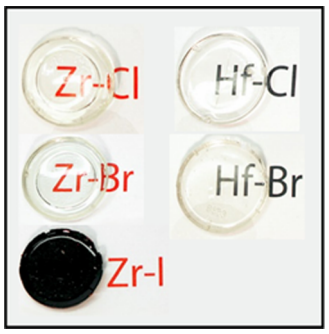

Figure 1. Hydroxohalide glasses prepared by evaporation. All specimens have $\alpha \approx 1$, except lower right, with $\alpha \approx 0.75$, and the Zr,I sample (see text). Disk diameter = 2.5 cm.

from the container walls. We observe different behavior for solutions with $\alpha < 0.7$. After about 2/3 of the water has evaporated, a clear voluminous gel forms, which upon further evaporation shrinks and then cracks extensively. The glass shards remain clear and are difficult to redissolve in water. For $\alpha \approx 0.5$, evaporation produces a white precipitate, which only partially dissolves in water. We regard $\alpha \approx 0.5$ to be the practical lower limit for glass formation.

We note that ZOC is known to lose water irreversibly on heating, beginning at $T \approx 45$ °C.[5] Therefore our syntheses, measurements, and discussion pertain to ordinary laboratory conditions of room temperature and relative humidity (RH), as opposed to "forcing" conditions such as heating, desiccation, or vacuum. These conditions preclude consideration of hydrates of ZOC with a small constitutional water content.

Figure 2 shows how the mass of a Zr,Cl specimen changes with RH. The observed mass change is fully reversible and

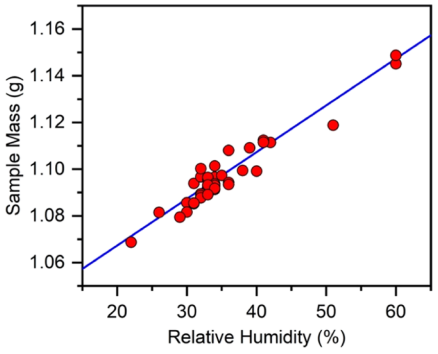

Figure 2. Mass (g) of a Zr,Cl glass ($\alpha \approx 1$) vs RH (%).

corresponds to approximately one water molecule over the span of RH from 20 to 60%. Humidity also affects the mechanical properties. Thin lamellae broken from a glass disk shrink and crack at low RH (~20%), fracture in "ordinary" humidity (30–50%), and become difficult to grind, as they plastically deform and tear above ≈60% RH. At room temperature, the corresponding bromide glasses deliquesce at about 75% RH and chloride glasses somewhat higher, about 90% RH. Placing the samples in a humidor at RH ≈ 100% results in complete liquefaction, producing a high-viscosity liquid when the weight gain reaches approximately 20%.

Figure 3 shows DSC and TGA scans for ZOC and a Zr,Cl glass ($\alpha \approx 1.1$). The trio of endothermic peaks at temperatures below 200 °C for ZOC in Figure 3a matches the mass-spectrometric signal for water loss reported by Scholz et al.[5]

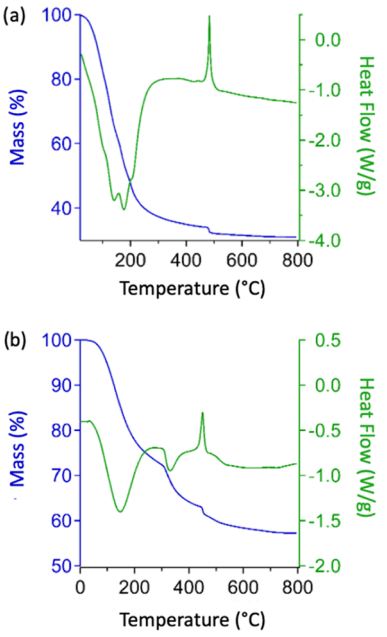

Figure 3. DSC-TGA of crystalline ZOC, (a) $\alpha = 2$ and (b) Zr,Cl glass, $\alpha \approx 1.1$.

The exothermic peak near 500 °C corresponds to crystallization of ZrO_2. Consequently, the total mass loss (66%) between room temperature and 500 °C corresponds to dehydration and loss of HCl.

The data in Figure 3b for the glass do not show simple melting. We characterize the thermal events as follows. Continuous loss of H_2O and HCl occur on heating to 300 °C and then vaporization of a portion, estimated at about 10%, of Zr as $ZrCl_4$ at its sublimation point of ≈330 °C. Blumenthal has noted similar volatilization of $ZrCl_4$. Since no oxygen-containing Zr species of the glass is volatile, the appearance of $ZrCl_4$ is significant because it shows that, in contrast to ZOC, Zr−Cl bonds are likely present in the glass or at least form early in the thermolysis. Near 450 °C, the sample crystallizes, coordinated with the loss of a small amount of H_2O and possibly HCl or $ZrCl_4$.

We choose to formulate crystalline MOX as $M(OH)_2X_2 \cdot 7H_2O$ and a general glass, M,X, as $M(OH)_{4-\alpha}X_\alpha \cdot nH_2O$. We also posit an ideal ($\alpha = 1$) formula for glasses: $M(OH)_3X \cdot 3H_2O$. Table 1 summarizes densities for crystalline phases calculated from crystallographic data and for glass counterparts measured by the Archimedean method. For comparison, we have included molar volumes for MOX phases from crystallographic data,[3,5] formula weights (FW) for MOX and ideal glass phases, and the number (n) of associated water molecules. It is evident that glass phases ($\alpha = 1$) are much denser than the crystalline form ($\alpha = 2$) for each halide. This increase in density is associated with the replacement of X^- by OH^- and a concomitant loss of constitutional water, i.e., a decrease in n. For Zr,Cl, we prepared a series of compositions to examine the glass homogeneity range for $\alpha < 1$ and to determine the effect of α on water content and molar volume (see Table 1). As α further decreases below 1, the water content continues to diminish, and the structure further densifies.

The hydriodic acid solution available to us was deeply colored, indicating an unknown degree of degradation to HI_3. Nonetheless, a good but dark glass sample, probably containing I_2, was formed (Figure 1). The iodide assay falls

https://doi.org/10.1021/acs.inorgchem.3c00633
Inorg. Chem. XXXX, XXX, XXX−XXX

Table 1. Composition and Density for Some M,X Glasses[1]

M,X	α	n	FW, g/mol	ρ, g/cm^3	$\tilde{V}$, cm^3/mol	RH, %
Zr,Cl						
ZOC[2]	2	7	323.1	1.896	170	
ideal	1	3	232.6			
	0.53	1.47	196	2.51	78	36
	0.58	1.59	200	2.60	77	28
	0.66	1.85	206	2.42	85	28
	0.70	1.57	201	2.59	78	<20
	0.76	2.06	211	2.42	87	34
	0.81	2.31	217	2.35	92	32
	0.87	2.30	218	2.47	88	32
	0.96	2.78	227	2.39	95	32
	0.96	3.80	246	2.27	109	42
	0.98	2.93	231	2.17	107	32
Zr,Br						
ZOB[2]	2	7	412.0	2.329	176.9	
ideal	1	3	277.1			
	0.91	2.82	268	2.59	103	33
Hf,Cl						
HOC[6]	2	7	409.4	2.439	167.9	
ideal	1	3	318.9			
	1.11	3.28	326	2.98	109	33
Hf,Br						
ideal	1	3	363.4			
	1.05	3.31	372	3.16	118	42
Zr,I						
ZOI[7]	2	7	505.2	2.697	187.3	
ideal	1	3	324.1			
	~0.5[#]		299	2.82	106	32

[1]Uncertainty estimates: α, 0.01; n, 0.3; FW, 5; ρ, 0.02; $\tilde{V}$, 3.5. Data for MOC phases from crystallographic sources.[2,6]

short of the expected value for α, possibly due to presence of elemental iodine.

Figure 4a,b graphs the number of water molecules and molar volumes vs α for all of the glasses in Table 1, excluding Zr,I. The linear relationships suggest that all M and X exhibit similar behavior, despite the range of anion sizes. The points that lie furthest from the fitted line were made at RHs appreciably different from ≈30%.

If in Figure 4a, we restrict attention to Zr,Cl points only, we find by linear least squares the equation $n_{H_2O} = 3.998\ (\pm 0.35)\alpha - 0.8573\ (\pm 0.17)$, with $R^2 = 0.7825$. This is the basis for our assertion of the formula $4\alpha - 1$ for n. Thus, n itself is implicitly determined by α. We note that this result also fits MOX and allows representation of all hydroxohalides as $M(OH)_{4-\alpha}X_\alpha \cdot (4\alpha - 1)H_2O$. We posit that this formula applies to all M,X but most evident for the longer series in Zr,Cl.

We have chosen to extend the density (ρ) and formula weight (FW) data to calculate molar volumes, $\tilde{V} = FW/\rho$. With the addition of halide per unit α, we are adding one (heavier) chloride ion but four lighter water molecules. Thus, density decreases with α, and $\tilde{V}$ increases. We can focus on $\tilde{V}$ to resolve the additive contributions from water molecules.

In similar fashion to the extrapolation of the n_{H_2O} data, we employ the molar volumes, $\tilde{V}$, to determine a $\tilde{V}_{ZOC}$ from glass data ($\alpha < 1$) and compare it to the crystallographic value of 170.4 cm^3. Thus, the extrapolation of the equation of Figure 4b, $\tilde{V} = 62.4\alpha + 40.8$ cm to $\alpha = 2$, gives $\tilde{V}_{ZOC}$ (from glass data) = 165.6 cm^3, showing good agreement with the crystallographic data. Furthermore, this model allows us to comment

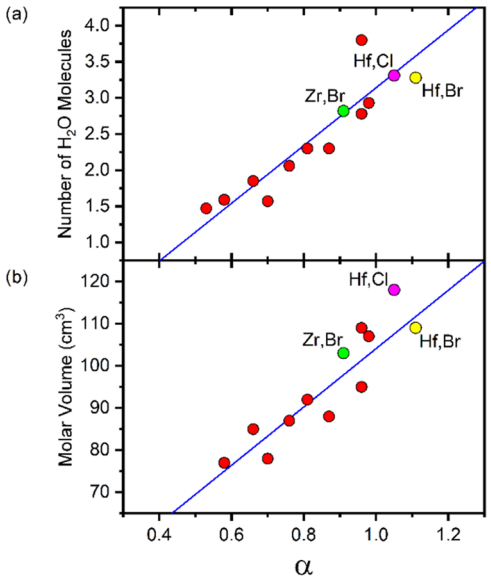

Figure 4. (a) Number of water molecules, n, and (b) the molar volume, cm^3, of glasses vs α for Zr,Cl glasses vs α, shown in red. Data points for Zr,Br; Hf,Cl; and Hf,Br are shown in green, magenta, and yellow, respectively. The fit line has been calculated for only the Zr,Cl data.

on possible porosity in the glasses. We can adjust the density of each glass sample by an assumed uniform porosity and recalculate $\tilde{V}$. Table 2 summarizes derived values of $\tilde{V}_{ZOC}$. The

Table 2. Estimated $\tilde{V}_{ZOC}$ as a Function of Glass Porosity

assumed porosity, %	$\tilde{V}_{ZOC}$
−10	150
0	166 ± 3.5
10	183
20	206

"−10%" line assumes the glasses are already 10% porous. Because the data suggest a significant deviation from the crystallographic data for glasses with porosity other than 0%, we surmise that the glasses exhibit negligible porosity.

We make further use of the density information. We calculate a contraction factor, defined as $(\tilde{V}_{glass}/\tilde{V}_{ZOC})^{1/3} = (\approx 110\ cm^3/170.4\ cm^3)^{1/3} \approx 0.86$, and draw a circle centered at the unit cell of ZOC[2] normal to the c-axis with radius = $0.86a_o/2\sqrt{2}$, as shown in Figure 5 (which is aligned along the c-axis). We see that it encloses four times the ideal glass formula of atoms, $Zr_4(OH)_8(H_2O)_{12}Cl_4$, or is written for the ideal glass formula, $Zr(OH)_3(H_2O)_3Cl$ (this count ignores the central Cl atom still pictured). We call this group the tetrameric motif. The three water molecules lost in this exclusion are just the three identified spectroscopically to leave in the 45−170 °C range,[5] mediated in our case by chemically exchanging chloride−hydrogen bonding for hydroxide−hydrogen bonding, instead of heating.

2.2. Observations on Phase Equilibria. As ZOC and HOC, $\alpha = 2$, are crystalline phases that transform to glasses with $\alpha \approx 1$, we undertook a study to determine the value α_{crit}, the smallest value at which the crystalline and glass phases coexist. Crystals of the familiar needle growth habit of ZOC were readily discerned, embedded in a glass matrix. By observing samples with crystal + glass (C + G) and glass (G)

https://doi.org/10.1021/acs.inorgchem.3c00633
Inorg. Chem. XXXX, XXX, XXX−XXX

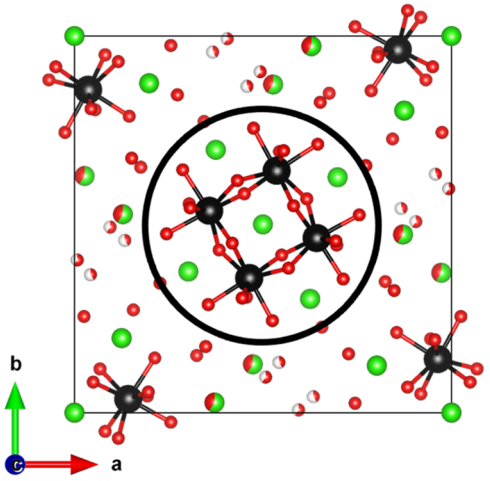

Figure 5. Unit cell of ZOC, with the circle of radius determined from the glass molar volume. Black, Zr; red, O; and green, Cl.

only, we deduced the α values listed in Table 3. Independently, we examined by powder XRD (see the Supporting Information) a series of compositions prepared by the ZBC method from C + G into G by X-ray powder diffraction, with α = 1.375, 1.25, and 1.125. For the series, the glass shows two weak, broad peaks due at d spacings of ≈3.37 and ≈2.14 Å. The hkl = 101 peak of ZOC at 7.03 Å was absent at α = 1.125, graphically determining α_{crit} = 1.15.

Table 3. Values of α_{crit} for Various M,X

M,X	α_{crit}, ±0. 03
Zr,Cl (ZBC)	0.99
Zr,Cl (ZBC) (XRD)	1.15
Zr,Cl (dialysis)	1.16
Hf,Cl (dialysis)	1.16
Zr, Br (ZBC)	0.98
Hf,Br (MOH + dialysis)	1.13

Values of α_{crit} for ZBC samples are somewhat smaller than those for dialysis of ZOC/HOC. Thus, two samples from ZBC at α = 1.04 and 1.00 were found to have a small fraction of crystals, but two samples from different dialysis runs produced only glass, with α's of 1.12 and 1.09. These results may suggest a difference in nucleation in the vicinity of α_{crit} based on the preparative method.

Evaporation products were found to be independent of steps or sequences of de- or re-acidification: if a glass producing solution, made either by ZBC or dialysis, is acidified with the appropriate amount of acid, it forms crystals, and if a crystal-producing solution by either method is brought into the glass region by dialysis, only glass is found. Furthermore, all solutions, ranging from ≈0.5 to 1.0 M, remain clear on timescales greater than 4 years. An exception was the Zr,I solution made from ZBC, which formed a gel upon standing for some weeks, possibly arising from oxidative degradation of the parent HI reagent noted above.

By the ZBC method, dissolution times become progressively longer with smaller α, leaving turbid solutions. Good glass samples have been obtained for $\alpha \approx 0.68$. This result parallels known behavior for slow neutralization of ZOC with base, wherein initial precipitation−redissolution shifts toward persistent insolubility and eventual gel formation with increasing base addition, which effectively decreases α.

2.3. Coexistence Diagram. Based on observations of evaporating solutions, we constructed Figure 6, a coexistence diagram of an aqueous, ternary isothermal section-type near T = 25 °C in which the three components are water (L), the crystalline phase (C,α = 2), and the glass phase (G,α = 1). We note that the last-listed choice of components is somewhat arbitrary as the glass region extends well below α = 1. As noted earlier, points on the diagram were determined under ambient laboratory conditions of t, RH. Though documented in Figure 2, slight variations of RH affect the water content but are unlikely to alter the invariant points and **S**. Table 4 summarizes

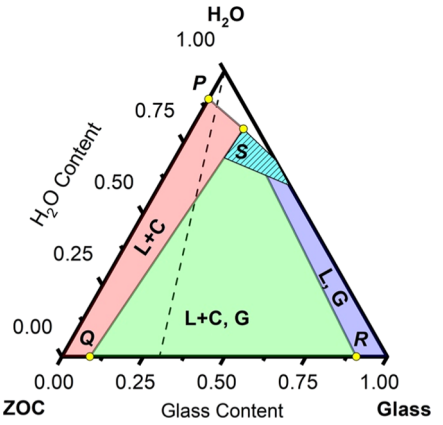

Figure 6. Isothermal coexistence diagram for water−crystal−glass.

Table 4. Mole Fractions of ZOC and Water for the Three Invariant Points and S

point	X_{ZOC}	X_{water}
P	0.11	0.89
Q	0.85	0
R	0.09	0
S	0.16	0.73

mole fractions of ZOC and water at these points. As to temperature, ZOC has a significant coefficient of solubility, so under temperatures elevated from 25 °C, the point **P** would be shifted downward, slightly enlarging the L-phase field and possibly **S** also since viscosity influences the judgment of "solidification".

The diagram is a schematic similar to an aqueous ternary phase diagram of water and two salts[7] with mutual solubility of the solid phases. We use this representation as a guide to evaporation phenomena in the present system. Points, **P**, **Q**, **R** are invariant. Point **P** is the solubility of ZOC in water. The α_{crit}'s (points **Q** and **R**) are the limits of solid solubility of each phase in the other; the determination of **Q** was found from X-ray diffraction of a Zr,Br sample, as explained in Section 2.5. For liquid compositions that evaporate to yield glasses, a gradual transition occurs from a viscous liquid to a hard solid within a narrow range of water loss, as opposed to a distinct equilibrium between liquid and solid phases. We indicate a shaded region within which the transition occurs. Therefore, point **S** cannot be considered an invariant. It was estimated with modest precision by visual observation, weighing, and penetration with a dissecting needle (to discern the "solid"

https://doi.org/10.1021/acs.inorgchem.3c00633
Inorg. Chem. XXXX, XXX, XXX−XXX

state) of a series of small samples during evaporation−humidification cycles. ***PS*** is thus the deliquescence line of ZOC and basic crystals. The phase fields are designated L + C for coexistence of the liquid and crystal, C + L,G for the coexistence of the crystal and liquid or solid glass, and L + G for the homogeneous phase. Evaporation follows a course similar to a conventional phase diagram: beginning near the top point of the triangle and descending along the dashed isopleth, crystals form from solutions initially in the L-phase field and to the left of the point ***S*** when the composition isopleth intersects ***PS***. Crystallization is followed by the formation of a glass phase; the reverse is true for solutions to the right of that point: crystals form inside a glass matrix when the isopleth crosses ***SR***. We estimate uncertainties of the various X_{H_2O} to be ±0.02, except for ***S***, where the difficulties of observing small quantities of liquid mixed with crystals justifies only ±0.05. We ignore lower hydrate(s) of ZOC, as noted above. When an isopleth reaches the ZOC-glass side (the "dry-up line" in conventional terminology), only "solid" phases are found. For solutions with compositions $\alpha \geq 1.84$, and with compositions $\alpha < 0.99$, only crystal and glass phases, respectively, are found. Adopting customary phase diagram usage, within the L + C, G two-phase field, the relative equilibrium amounts of the crystal and glass are given by the lever rule at the composition point on the ZOC, glass axis. In the XRD series, the strong presence of ZOC was found at α = 1.375, but this observation was not further quantified.

2.4. Solution Species. SWAXS analyses of solutions provide a means to elucidate speciation at selected values of α. We performed the measurements on solutions approximately 1 M in metal. Figure 7 shows scattering curves for solutions that

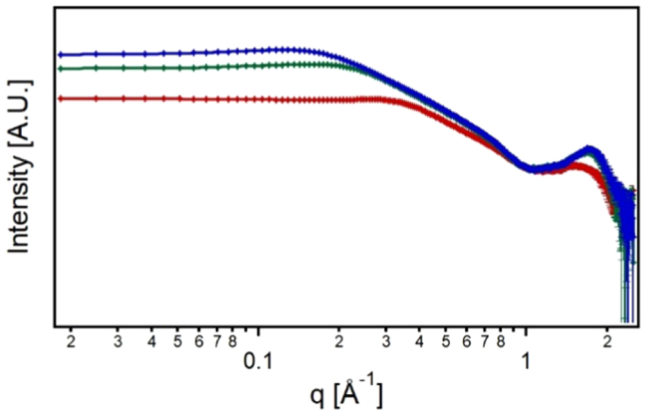

Figure 7. Scattering curves for ZBC systems exhibiting an increase in cylindrical length from crystal to glass formers. Red: crystal (α = 2), green: glass + crystal (α = 1.2), and blue: glass (α = 1).

produce crystal (α = 2), glass + crystal (α = 1.2), and glass (α = 1). The onset of the negative slope in each curve shifts to small q in the order α = 2, α =1.2, and α = 1. The curves indicate larger species form as α decreases, consistent with increasing condensation across the series as OH^- replaces Cl^-.

Table 5 summarizes modeled structural parameters from pair distribution function (PDDF) analyses and Irena macros of Zr solution prepared by the ZBC method. As α decreases, the radius of gyration (R_g) increases from 3.6 Å (α = 2) to 7.7 Å (α = 1). Heating the α = 1 solution increases R_g further to 13.2 Å. Therefore, R_g provides a simple summary of increasing species size based on forced condensation.

Table 5. Modeled Values from PDDF Analysis and Modeling II in Irena Macros

	R_g—PDDF (Å)	max linear ext—PDDF (Å)	radius from cylindrical fit (Å)	length from cylindrical fit (Å)
		ZBC		
α = 2.0 (crystal)	3.6	10	3.0	10.3
α = 1.2	5.9	17	3.6	16.5
α = 1.0 (glass)	7.7	24	3.9	22.2
α = 1.0 (thermal)	13.2 Å (spherical radius)			
simulated octamer[1]	4.3	13.5	2.7	13.5

The radius and length of a cylindrical fit of the data for α = 2 approximate a simulated octamer (see Table 5). The maximum linear distance from the PDDF provide additional support for the proposed speciation. The discrepancies between the measured and simulated values may arise from (1) interactions between scattering species giving rise to a Coulombic peak known as a structure factor, which complicates modeling or (2) a mixture of tetrameric and octameric species that produces shorter distances. Diluting the solution does not affect the scattering curve or the derived results.

The Zr crystal forming solution (α = 2) contains scattering species in agreement with cylindrical species composed of two tetramers linked side by side. The glass forming solutions (α = 1) indicate longer lengths corresponding to four linked tetramers. The mixed crystal/glass forming systems (α = 1.2) contain an intermediate species of three linked tetramers. The trend of the shift of the Guinier region (near where the curve begins to decrease with Q) from higher to lower Q (smaller to larger particles) in going from crystal forming to glass forming indicates longer chain formation (see Figure 7).

The solution with entry "thermal" in Table 5 was held at 90 °C for 96 h. The result stands out for its indication of extensive polymerization (see Figure 8). The SWAXS analysis of this

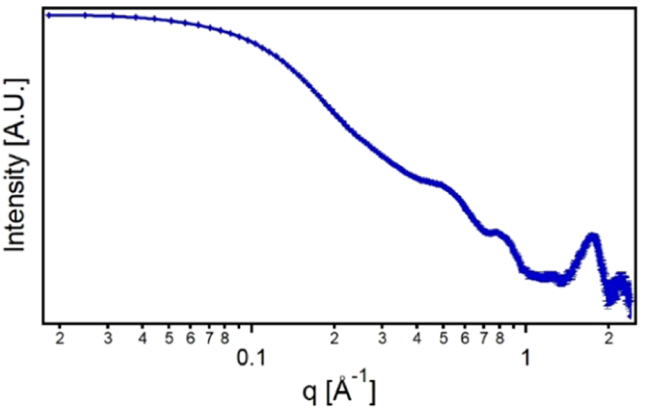

Figure 8. Scattering curve for heated ZBC solution, α = 1.

solution indicated a polydisperse mixture, primarily composed of spherical nanoparticles with a radius of 13.2 Å. This is consistent with the finding of Clearfield[8] for prolonged reflux of partially neutralized ZOC solutions, which produced monoclinic ZrO_2. Based on his analysis of particle size, he indicated that 48−96 monomer units of ZrO_2 may be "the upper limit of the size of the polymers obtained in solution." If

https://doi.org/10.1021/acs.inorgchem.3c00633
Inorg. Chem. XXXX, XXX, XXX−XXX

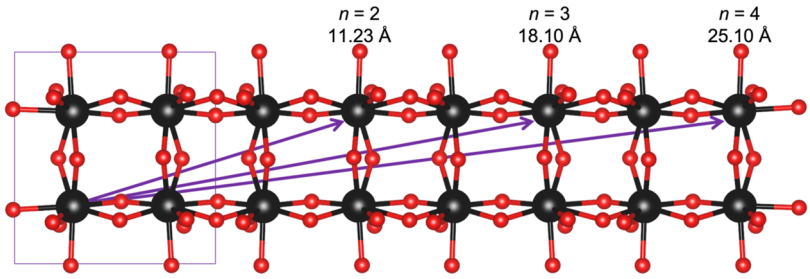

Figure 9. Proposed model for two tetrameric units linked by bridging hydroxides: black, Zr and red, O.

we convert the implied radius of 13.2 Å into a Zr number using the contracted crystallographic formula unit volume of (110 $cm^3 \cdot E24/N_A$) = 183 $Å^3$, we estimate that these idealized spheres contain about $(4/3) \times \pi \times (13.2)^3/183 \approx 53$ such units.

The above findings suggest a very simple model based on the side-way linking of tetramer units into di-, tri-, and quadrimers, containing 8, 12, and 16 Zr atoms, using only one parameter, the Zr−Zr crystallographic distance (through bridging hydroxide pairs) of 3.55 Å. The Zr−Zr diagonal lengths, d, of this series, whose dimer member is shown in Figure 9, are given by $d = 3.55\sqrt{1 + (2n - 1)^2}$, for n = 2, 3, and 4. This determines d's of 11.23, 18.10, and 25.10 Å, to be compared with the max linear ext (10, 17, 24 Å) or length (10.3, 16.5, 22.2 Å) from cylindrical fit columns of Table 5. This model makes no account of scattering contributions of Cl, O atoms. Our Figure 9 is identical to the right-hand column of Figure 5 of ref 9.

In the polymerization reactions, e.g., for formation of the dimer

$$2Zr_4(OH)_8(H_2O)_{16}^{8+} \rightleftarrows Zr_8(OH)_{20}(H_2O)_{24}^{12+} + 4H^+ + 4H_2O$$

four new bridging hydroxide bonds are formed between the tetrameric units, and four protons are liberated. We presume that the mechanism in, e.g., dialysis, is that the diffusing HX consists of a proton furnished by ionization of a water molecule attached to Zr, which becomes a bridging hydroxide and a halide ion. Polymerization reactions will be shifted to the right by influences such as dialysis and neutralization.

Several articles have covered different aspects of solution species in related systems. There is consistency with work[10] on HOC with α = 2, at lower concentrations, where a sheet octamer (dimer of tetrametric units) is found; and at higher concentrations (500 mM), a tetramer with a radius of gyration, R_g, of 3.5−4 Å is found. With synchrotron source radiation, Singhal and co-workers[11] find for ZOC at varying pHs, R_g of 3.8Å for the tetramer and 5.1 Å for the octamer, and an increase of R_g as pH increases. They interpret their scattering data with a tetrameric unit of formula $Zr_4(OH)_8(H_2O)_{16}Cl_6^{2+}$ and an octameric (like our dimer-of-tetramers, but with side-by-side and stacked options, with slight favor of the latter) unit of formula $Zr_8(OH)_{20}(H_2O)_{24}Cl_{12}$, with an equilibrium between the two favoring the latter at higher pH. Åberg[12] has measured total X-ray scattering on solutions of ZOC and HOC (prepared by hydroxide dissolution) with α = 1 and 2. For the former, scattering curves are interpreted as the tetramer and the latter as "randomly formed polymers" of an unknown degree.

We conclude that SWAXS results are independent of the preparative method for the Zr,Cl solutions; results for Zr and Hf solutions are also similar. Soaking at 90 °C gives rise to extensive condensation and larger species.

2.5. Basic Hydroxohalide Crystal Structure. At least three X-ray diffraction studies have been reported for ZOC,[3,13,14] each identifying the tetrameric unit of Zr atoms connected by bridging hydroxides. Four water molecules bind to each Zr atom with three more present constitutionally to form a hydrogen-bond network. Studies place a chloride ion just above the center of the tetramer; one chloride partially occupies its site to arrive at α = 2. For ZOC, we review the α count. The occupancy of the three chloride positions, Cl(1), Cl(2), and Cl(3) are 1, 1, and 0.75, respectively (these positions can be seen in the equivalent ZOB basic crystal in Figure 10). Cl(1) is at a special position so that its two

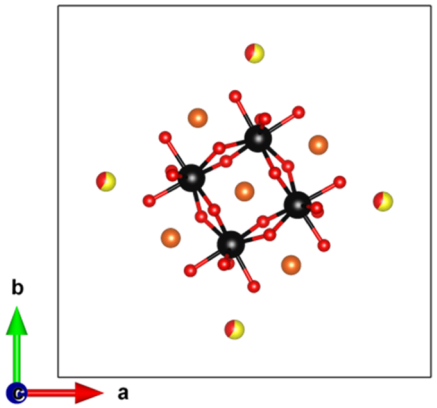

Figure 10. Tetrahedral unit of zirconium hydroxobromide, viewed down the crystallographic c-axis, with partial hydroxide substitution of bromide positions. Black, Zr; red, oxygen; orange, bromide positions Br (1) and Br (2); and yellow-red bromide, position Br (3), partially substituted by hydroxide.

symmetrically equivalent atoms belong to eight unit cells; Cl(2) and Cl(3) are within the asymmetric unit. Therefore, $\alpha = 2 \times (1/8) \times 1 + 1 \times 1 + 1 \times (0.75) = 2$.

Of primary interest to basic hydroxohalides is the question what structural accommodation occurs as X^- is replaced by the smaller and more basic OH^- but not yet sufficiently to form glass exclusively? We prepared crystal assemblages C + G, in a condition where crystals could be taken from a partially liquid matrix for both Zr,Cl and Zr,Br. It was found more favorable to use the Zr,Br assemblage. A suitable single crystal was recovered from a mixture with bulk composition α = 1.09 and analyzed. We found the expected space group, $P\bar{4}2_1c$ (114), with the same arrangement of atoms, i.e., the tetramer of OH-bridged Zr atoms. The Br(3) position, analogous to the

https://doi.org/10.1021/acs.inorgchem.3c00633
Inorg. Chem. XXXX, XXX, XXX−XXX

Cl(3) position discussed above for ZOC, was found to be equally and partially occupied (0.594) by Br and partially by O (0.406), with Br(1) and Br(2) still fully occupied. Full details of the structure are found in Tables S1 and S2. Therefore, $\alpha = 2 \times (1/8) \times 1 + 1 \times 1 + 1 \times 0.594 = 1.844$. Because of the similarities of ZOC and ZOB, we have used this bromide-derived point as **Q** in Figure 6.

The structure of Figure 10 compares to the circled region of the ZOC motif in Figure 5, which was estimated from a molar volume calculation. It appears that the tetrameric core is retained. As α decreases to 1, Cl^- continuously replaces OH^- to produce a sea of Cl^- ions and short Zr−Cl distances, i.e., 3.5 Å, compared with 4.5−4.6 Å in crystalline ZOC. This short Zr−Cl distance is consistent with the observed vaporization of $ZrCl_4$ at elevated temperatures.

3. CONCLUSIONS

Among the basic hydroxohalide glasses obtained by evaporation of aqueous solutions, very similar behavior is found for both Zr and Hf and for anions Cl and Br, which likely extends to I as well. This similarity is found for each of the three phases studied: solution, basic crystal, and glass. The glass and crystal phases coexist over a wide range of α. The glass phases are denser than their crystalline counterparts, based on replacement of hydroxide for halide and concomitant decrease in constitutional water content. The lower limit for glass formation is $\alpha \approx 0.5$, below which extensive hydrolysis to insoluble hydrous oxide−hydroxide occurs. Formulas for compositions in the glass homogeneity range can be written as a function of the single parameter, α. The tetrameric motif $[M_4(OH)_8]^{8+}$ is found in each of the three phases with condensation of these units increasing as α decreases.

■ ASSOCIATED CONTENT

Supporting Information

The Supporting Information is available free of charge at https://pubs.acs.org/doi/10.1021/acs.inorgchem.3c00633.

Refined positional parameters and anisotropic displacement coefficients for ZOB (PDF)

Accession Codes

CCDC 2061005 contains the supplementary crystallographic data for this paper. These data can be obtained free of charge via www.ccdc.cam.ac.uk/data_request/cif, or by emailing data_request@ccdc.cam.ac.uk, or by contacting The Cambridge Crystallographic Data Centre, 12 Union Road, Cambridge CB2 1EZ, UK; fax: +44 1223 336033.

■ AUTHOR INFORMATION

Corresponding Author

Douglas A. Keszler − *Department of Chemistry, Oregon State University, Corvallis, Oregon 97331-4003, United States;* orcid.org/0000-0002-7112-1171; Email: douglas.keszler@oregonstate.edu

Authors

James A. Sommers − *Department of Chemistry, Oregon State University, Corvallis, Oregon 97331-4003, United States*

Jenn M. Amador − *Department of Chemistry, Oregon State University, Corvallis, Oregon 97331-4003, United States*

Lauren B. Fullmer − *Department of Chemistry, Oregon State University, Corvallis, Oregon 97331-4003, United States*

Danielle C. Hutchison − *Department of Chemistry, Oregon State University, Corvallis, Oregon 97331-4003, United States*

T. Wesley Surta − *Department of Chemistry, Oregon State University, Corvallis, Oregon 97331-4003, United States;* Present Address: Department of Chemistry, University of Liverpool, Liverpool L69 7ZD, United Kingdom

Oksana Ostroverkhova − *Department of Chemistry, Oregon State University, Corvallis, Oregon 97331-4003, United States*

May Nyman − *Department of Chemistry, Oregon State University, Corvallis, Oregon 97331-4003, United States;* orcid.org/0000-0002-1787-0518

Complete contact information is available at: https://pubs.acs.org/10.1021/acs.inorgchem.3c00633

Notes

The authors declare no competing financial interest.

■ ACKNOWLEDGMENTS

This material is based upon work supported by the National Science Foundation under Grant No. CHE-1606982. The authors thank Dr. Lev N. Zakharov for the X-ray structure determination, Dr. Sumit Saha for DSC/TGA measurements, and Eaton C. Fong for assistance with graphics.

■ REFERENCES

(1) Nielsen, R. H.; Schlewitz, J. H.; Nielsen, H. Zirconium and Zirconium Compounds. In *Kirk-Othmer Encyclopedia of Chemical Technology*, 3rd ed.; John Wiley & Sons, Inc.: New York, NY, 1984; Vol. *24*, p 863.

(2) Clearfield, A.; Vaughan, P. A. The Crystal Structure of Zirconyl Chloride Octahydrate and Zirconyl Bromide Octahydrate. *Acta Crystallogr.* **1956**, *9*, 555−558.

(3) Blumenthal, W. B. *The Chemical Behavior of Zirconium*; D. Van Nostrand Company, Inc.: Princeton, NJ, 1958; p 132.

(4) Endemann, H. Lösliche basisiche Zirkonerdesalze. *J. Prakt. Chem.* **1875**, *11*, 219−222.

(5) Scholz, J.; Scholz (nee Böhme), K.; McQuillan, A. J. In Situ Infrared Spectroscopic Analysis of the Water Modes of $[Zr_4(OH)_8(H_2O)_{16}]^{8+}$ during the Thermal Dehydration of $ZrOCl_2 \cdot 8H_2O$. *J. Phys. Chem. A* **2010**, *114*, 7733.

(6) Sinram, D.; Krebs, B. Tetranuclear $[Zr_4(OH)_8(H_2O)_{16}]$ units in the crystal structure of $ZrOI_2 \cdot 8H_2O$. *Z. Kristallogr.* **2005**, *220*, 166−168.

(7) Findlay, A. *The Phase Rule and Its Applications*; Dover Publications, Inc.: New York, NY, 1951; p 377.

(8) Clearfield, A. Crystalline Hydrous Zirconia. *Inorg. Chem.* **1964**, *3*, 146−148.

(9) Kalaji, A.; Skanthakumar, S.; Kanatzidis, M. G.; Mitchell, J. F.; Soderholm, L. Changing Hafnium Speciation in Aqueous Sulfate Solutions: A High-Energy X-ray Scattering Study. *Inorg. Chem.* **2014**, *53*, 6321−6328.

(10) Ruther, R. E.; Baker, B. M.; Son, J.-H.; Casey, W. H.; Nyman, M. Hafnium Sulfate Prenucleation Clusters and the Hf_{18} Polyoxometalate Red Herring. *Inorg. Chem.* **2014**, *53*, 4234.

(11) Singhal, A.; Toth, L. M.; Lin, J. S.; Affholter, K. Zirconium(IV) Tetramer/Octamer Hydrolysis Equilibrium in Aqueous Hydrochloric Acid Solution. *J. Am. Chem. Soc.* **1996**, *118*, 11529−11534.

(12) Åberg, M. An X-ray Investigation of Some Aqueous Zirconium (IV) Halide, a Hafnium (IV) Chloride, and Some Zirconium (IV) Perchlorate Solutions. *Acta Chem. Scand., Ser. A* **1977**, *31*, 171−181.

(13) Mak, T. C. W. Refinement of the crystal structure of zirconium chloride octahydrate. *Can. J. Chem.* **1968**, *46*, 3491−3497.

(14) Hagfeldt, C.; Kessler, V.; Persson, I. Structure of the hydrated, hydrolysed and solvated zirconium (IV) and hafnium (IV) ions in

water and aprotic oxygen donor solvents. A crystallographic, EXAFS spectroscopic and large angle X-ray scattering study. *Dalton Trans.* **2004**, 2142−2153.

https://doi.org/10.1021/acs.inorgchem.3c00633
Inorg. Chem. XXXX, XXX, XXX−XXX